Coupling of molecular vibrons with contact phonon reservoirs

2007 J. Phys.: Condens. Matter 19 215207

(http://iopscience.iop.org/0953-8984/19/21/215207)

IOP PUBLISHING JOURNAL OF PHYSICS: CONDENSED MATTER

J. Phys.: Condens. Matter **19** (2007) 215207 (12pp) doi:10.1088/0953-8984/19/21/215207

Coupling of molecular vibrons with contact phonon reservoirs

G Romano, A Pecchia and A Di Carlo

Department of Electronics Engineering, University of Rome 'Tor Vergata', Via del Politecnico 1, 00133, Roma, Italy

E-mail: pecchia@ing.uniroma2.it

Received 28 December 2006, in final form 9 March 2007
Published 1 May 2007
Online at stacks.iop.org/JPhysCM/19/215207

Abstract

In this paper we describe a computational method for coupling localized molecular vibrations with contact phonons using a Green's function formalism. The phonon Green's function is constructed from the dynamical matrix of the *contact–molecule–contact* coupled system. Within this formalism we identify the imaginary part of the self-energy as the vibron lifetime for decay into contact phonons. This first-principles calculation allows us to compute the microscopic energy dissipation and the heat transport from the molecule to the contacts. This is a fundamental step for the evaluation of the power dissipated in molecular devices and for studying the thermal stability of molecular devices.

(Some figures in this article are in colour only in the electronic version)

1. Introduction

The feasibility of molecular electronics as a viable future technology critically depends on the stability of the compounds under bias conditions. Local heating is, among others, a crucial quantity to be accurately evaluated to assess molecular stability and guide device optimizations. Noticeably, current-induced local heating in a molecular junction made of octane-dithiol has been measured for the first time recently [1]. Many models and theories have been developed in recent years to account for electron–vibron scattering and heat dissipation in nanojunctions. For an extended review on the subject see [2]. A crucial parameter for the computation of the molecular heating is the rate of phonon dissipation into the reservoirs. Most models include electron–vibration coupling and phonon release in molecular bridges and account for phonon dissipation into the heat reservoirs by introducing phenomenological parameters [3–6].

In this work we consider a *contact–molecule–contact* system and, imposing open boundary conditions on the atomic vibrations, provide a prediction of the decay rates of the molecular *phonons* into the reservoirs. The calculation is based on a first-principles method, including the elastic coupling of molecular modes with contact vibrations.

In the first section we define the theory framework of the Green's function formalism applied to vibrations, which allows us to treat open boundary conditions. The method is used to define the local density of states projected on the molecule and the phonon decay rates on the contact reservoirs. This approach, coupled with a self-consistent rate equation, allows us to define the out-of-equilibrium phonon populations of the junctions under bias conditions and the local heating of the molecule. An application to two molecular systems comprising a benzene molecule bridging two Si contacts is presented. The two systems differ in the Si–C bond configuration, which is reflected in a large difference of the coherent tunnelling current as well as the incoherent electron–phonon scattering and eventually local heating.

2. Theory

The atomic vibrations of the open structure are treated in the usual way [7–10], after decoupling the Hamiltonian as a superposition of normal modes of vibration. The modes and frequencies for the whole structure are obtained by solving the eigenvalue system

$$\sum_j \mathcal{H}_{ij} e_j^p = \sum_j \mathcal{M}_{ij} e_j^p \omega_p^2, \tag{1}$$

where e_j^p are the normal modes, and $\mathcal{M}_{ij}$ and $\mathcal{H}_{ij}$ are the mass and Hessian matrices, respectively. The mass matrix is a diagonal matrix containing the atomic masses and the Hessian matrix is defined using the Hellmann–Feynman theorem as

$$\mathcal{H}_{\alpha,\beta} = \frac{\partial^2 E}{\partial R_\alpha \partial R_\beta}, \tag{2}$$

where E is the total energy of the system. The practical problem posed by equation (1) is that the contacts are semi-infinite and consequently the matrices $\mathcal{H}_{ij}$ and $\mathcal{M}_{ij}$ have infinite dimension.

In order to treat the open boundary conditions on the bulk side of the contacts we use the Green's function formalism. The treatment is analogous to the electronic Green's functions, usually defined in quantum transport problems [11]. We start by defining the Green's function corresponding to equation (1) and partition the system into molecule and contact blocks. For instance, restricting ourselves to the left contact only, the following equation can be written for the Green's function:

$$\begin{bmatrix} \mathcal{M}_{\mathrm{M}}\omega^2 - \mathcal{H}_{\mathrm{M}} & \mathcal{H}_{\mathrm{M,L}} \\ \mathcal{H}_{\mathrm{L,M}} & \mathcal{M}_{\mathrm{L}}\omega^2 - \mathcal{H}_{\mathrm{L}} \end{bmatrix} \begin{bmatrix} G^r_{\mathrm{M}} & G^r_{\mathrm{M,L}} \\ G^r_{\mathrm{M,L}} & G^r_{\mathrm{L}} \end{bmatrix} = \begin{bmatrix} I & 0 \\ 0 & I \end{bmatrix}. \tag{3}$$

The matrix blocks are obtained from the computation of the Hessian of the whole system. The labels M and L stand for the molecular and the left contact blocks, respectively. In practice a particular treatment must be taken for the contacts, since the calculation of the Hessian must be performed on a finite system. Our strategy is to compute the Hessian for a truncated system that includes a sufficiently large portion of the contacts. In each contact we can identify a surface and a bulk, comprising two principal layers (PLs) which are chosen in order to satisfy the condition that the Hessian matrix appears block-tridiagonal, i.e., the elastic coupling does not extend beyond nearest-neighbour PLs. Hydrogen saturation or a buffer layer can be included to terminate the cut edge at the bulk sides of each contact. The diagonal blocks of the Hessian, corresponding to the PLs, and the coupling blocks between PLs are replicated an infinite number of times, corresponding to the definition of an ideal bulk. Care is taken to ensure converged results by increasing the PL size. The Green's function is defined in the usual form,

$$G^r(\omega^2) = \frac{1}{\mathcal{M}_{\mathrm{M}}\omega^2 - \mathcal{H}_{\mathrm{M}} - \Pi^r_{\mathrm{R}}(\omega^2) - \Pi^r_{\mathrm{L}}(\omega^2)}, \tag{4}$$

where the self-energies, $\Pi^r_{\mathrm{L,R}}(\omega^2)$, exactly map the infinite left and right contacts into the finite portion of the molecular subsystem. Atomic units ($\hbar = 1$) are used throughout. In the Green's function (4) we keep the explicit dependence on ω^2, as expressed in the corresponding eigensystem (1). The self-energies are obtained from equation (3) as

$$\Pi^r_{\mathrm{L}}(\omega^2) = \mathcal{H}_{\mathrm{M,L}} g^r_{\mathrm{L}}(\omega^2) \mathcal{H}_{\mathrm{L,M}}, \tag{5}$$

where g^r_{L} represents the surface Green's function of the left semi-infinite contact, defined as

$$g^r_{\mathrm{L}}(\omega^2) = \frac{1}{\mathcal{M}_{\mathrm{L}}\omega^2 - \mathcal{H}_{\mathrm{L}}}. \tag{6}$$

This is computed using a recursive algorithm [12] from the knowledge of the PL blocks defined above. The local phonon density of states (LDOS) projected on the molecule can be computed from $G^r(\omega^2)$ by means of the expression

$$\rho(\omega^2) = -\frac{1}{\pi}\mathrm{Tr}\left\{\mathrm{Im}\left[G^r(\omega^2)\right]\mathcal{M}\right\}. \tag{7}$$

This quantity is also expressed in terms of ω^2. The connection with the usual DOS can be recovered using the function derivative

$$\rho(\omega) = \frac{\partial N}{\partial \omega} = 2\omega\rho(\omega^2) = -\frac{2\omega}{\pi}\mathrm{Tr}\left\{\mathrm{Im}\left[G^r(\omega^2)\right]\mathcal{M}\right\}. \tag{8}$$

The frequencies and modes of the molecule interacting with the contacts can be obtained by solving the eigensystem

$$\sum_j \left[\mathcal{H}_{\mathrm{M},ij} + \Pi^r_{ij}\left(\omega^2\right)\right]\phi^q_j = \sum_j \omega^2_q \mathcal{M}_{ij}\phi^q_j. \tag{9}$$

In principle this equation can give exact eigenvectors, ϕ^q, and frequencies, ω_q, but it is rather impractical to solve because of the nonlinear terms given by the complex self-energies. For this reason it is often useful to take a first-order expansion of (9) which approximates the exact eigenvectors of the coupled system with those of the uncoupled molecule, e^q, satisfying the equation

$$\sum_j \mathcal{H}_{\mathrm{M},ij} e^q_j = \sum_j \mathcal{M}_{\mathrm{M},ij} e^q_j \omega^2_q, \tag{10}$$

whereas the mode frequencies are given by

$$\bar{\omega}^2_q = \omega^2_q + \mathcal{Z}_q \sum_{ij} e^q_i \,\mathrm{Re}\left[\Pi^r_{ij}(\omega^2_q)\right] e^q_j, \tag{11}$$

where

$$\mathcal{Z}_q = \left[1 - \sum_{ij} e^q_i \left.\frac{\partial\,\mathrm{Re}\left[\Pi^r_{ij}(\omega^2)\right]}{\partial\omega^2}\right|_{\omega=\omega_q} e^q_j\right]^{-1}. \tag{12}$$

In practice this approximation gives new, renormalized, frequencies and associated broadenings, reflecting the interaction with the contact reservoirs. The mode broadening is related to the imaginary part of the self-energy by

$$\Gamma_q = \sum_{ij} e^q_i \,\mathrm{Im}\left[\Pi^r_{ij}(\omega^2_q)\right] e^q_j. \tag{13}$$

The connection between broadening and the phonon decay rate can be obtained starting from the usual representation of the Green's function on the basis of the eigenmodes,

$$\tilde{G}_q(\omega) = \frac{1}{\omega^2 - \bar{\omega}^2_q - \mathrm{i}\Gamma_q} \cong \frac{1}{2\bar{\omega}_q(\omega - \bar{\omega}_q) - \mathrm{i}\Gamma_q}, \tag{14}$$

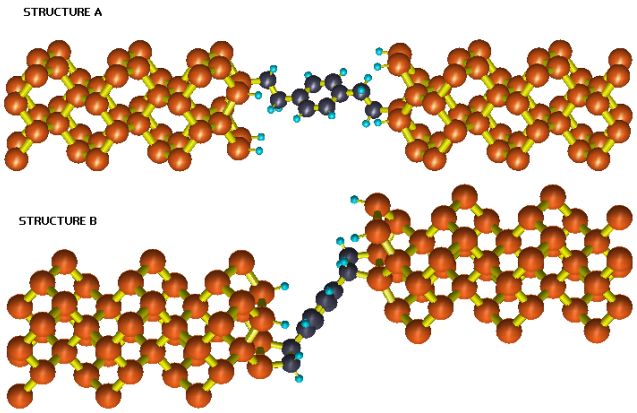

Figure 1. Hybrid structures comprising two semi-infinite contacts of hydrogenated Si(100), reconstructed 2 × 1, and adsorbed organic molecules.

and the spectral density in terms of the Green's function

$$\tilde{\rho}(\omega) = -\frac{2\bar{\omega}_q}{\pi} \sum_q \mathrm{Im}\left[\tilde{G}_q(\omega)\right] \cong -\frac{1}{\pi} \sum_q \frac{\frac{\Gamma_q}{2\bar{\omega}_q}}{\left(\omega - \bar{\omega}_q\right)^2 + \left(\frac{\Gamma_q}{2\bar{\omega}_q}\right)^2} \tag{15}$$

which leads, using the relationship $\tau^{-1} = -2\,\mathrm{Im}[\Sigma]$ between lifetime and self-energy, to the identification of $J_q = -\frac{\Gamma_q}{\bar{\omega}_q}$ as the phonon decay rates.

The method implemented is essentially a Fermi golden rule, including first-order one-phonon-to-one-phonon decay processes, but it obviously neglects a large number of other mechanisms that may take place when the direct decay is forbidden. High-frequency modes, characteristic of molecular vibrations, generally lie well beyond the vibrational bandwidth of the bulk reservoirs and cannot decay other than via one-to-many phonon channels [13, 14]. Some of these effects can be taken into account by introducing effective phonon densities for the contact modes [15]. This, for instance, allows the correct prediction of the temperature dependence of many-phonon decay rates. However, quantitative predictions of one-phonon-to-many-phonons decay rates require the calculation of coupling constants related, for instance, to anharmonic potentials, not explicitly treated in this work. Other decay mechanisms may also be represented by vibrational coupling with the surrounding molecules, which generally depends on the environment, or with multistep processes involving relaxations to lower-energy modes via anharmonic couplings. Radiative decays may also play an important role in some specific molecules.

3. Numerical simulation

The method has been applied to two systems (see figure 1) obtained by a sandwich of an organic layer between two Si contacts. The contacts of both structures are identical and made of hydrogenated Si(100), 2 × 1 reconstructed. The molecules are adsorbed on the surface via Si–C covalent bonds. For the first system the molecule chosen is $C_{10}H_{12}$ (structure A), whereas $C_{10}H_{10}$ is used in the second structure (structure B). Periodic boundary conditions are imposed in the direction parallel to the Si surfaces on both structures.

The total energy of the contact–molecule–contact system is obtained through a local basis density functional scheme, where appropriate approximations are considered in order to make

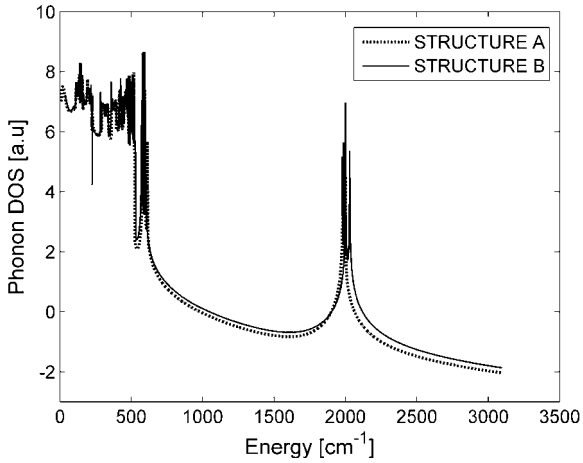

Figure 2. Phonon DOS of the contacts.

the approach efficient for a large number of atoms (DFTB) [16–18]. These include the use of an optimized minimal basis set and the neglect of three-centre integrals. Both the electronic and the repulsive potential are expressed as a superposition of atomic pair-potentials, obtained from *ab initio* density functional theory (DFT) reference calculations [18] allowing extensive use of look-up tables. The method is very successful in describing structural properties of materials and also gives accurate results for the mode frequencies.

4. Projected DOS

We have seen how the contacts induce a perturbation on the molecular modes and vibrational frequencies. Additionally, we have obtained two approaches for the evaluation of the projected DOS. The first method gives the exact DOS as obtained from the exact Green's function of the open system, defined in equation (8). In the second method the self-energies are approximated by an energy-independent shift and broadening, leading to the form of equation (15). For vanishing coupling ($\Pi^r(\omega^2) \rightarrow 0$) the DOS tends to a superposition of delta-functions. This happens for frequencies quite above the Si bandwidth.

The left and right contacts are identical and therefore the phonon bandwidths are the same. The projected phonon DOS on the contact surface is shown in figure 2. This is obtained from the surface Green's function of equation (6). The frequency cutoff (ω_D) is about 500 cm^{-1}, appropriate for bulk Si. The peaks around 580 and 2000 cm^{-1} are related to the hydrogen passivation of the silicon surface.

The projected phonon DOS on the molecule is represented in figure 3. The figure shows a comparison between the exact and the approximated DOS up to the Si cutoff frequency. Obviously the simple *shift* + *broadening* approximation is sometimes too crude and does not capture the richness of the exact result. However, it gives a first-order approximation to the complex problem of defining the vibrational lifetimes.

5. Phonon decay rates

The phonon decay rates, J_q, of both structures are computed using equation (13) and are shown in figure 4. Qualitatively similar results are obtained, which strongly depend on the contact DOS. Indeed, J_q is fast for the energy modes lying within the contact phonon bandwidth

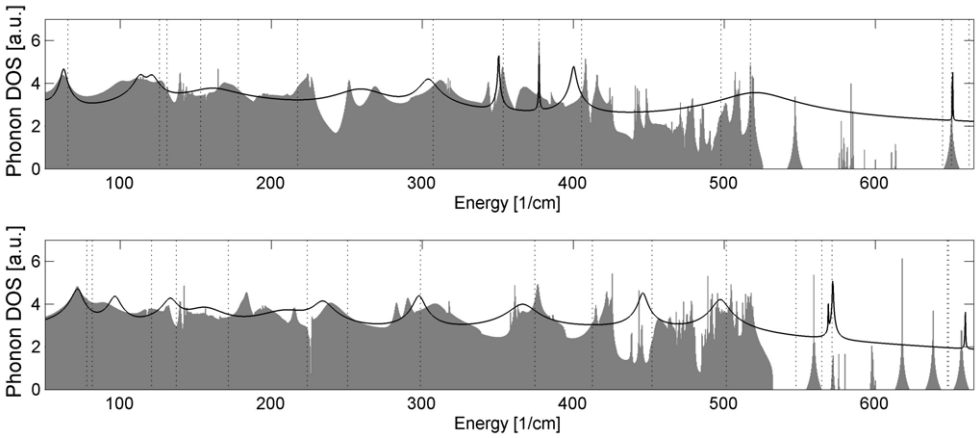

Figure 3. Phonon DOS projected on the molecule. The dashed lines correspond to the unperturbed molecular frequencies. The solid line is the lowest-order approximated DOS and the grey shaded area represents the exact DOS.

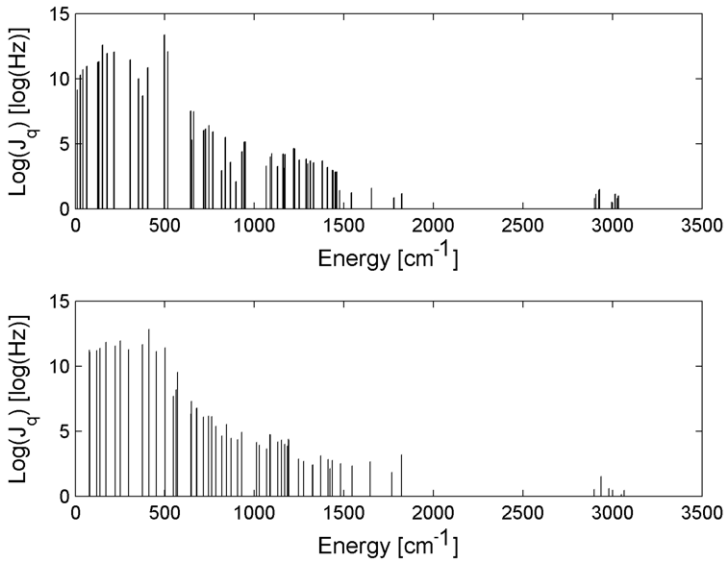

Figure 4. Decay rates of the molecular vibrons into contact phonons.

and sharply decreases beyond, reaching very small values. These decays are likely to be underestimated, as discussed in the previous section, because they do not include anharmonic corrections that generate one-phonon-to-many-phonons decay channels.

Despite the difference in nature of the Si–C bonds between the two systems considered (one bond Si–C for structure A and two bonds for structure B), the decay rates have similar trends and magnitudes. Due to its higher number of bonds to the surface and shorter length, molecule B is more rigid and passes higher mode frequencies. For this reason the elastic coupling to the surface is slightly more effective with respect to molecule A, as also seen in figure 4. Indeed, the lowest-frequency modes of structure B have rates at least twice as large as those of structure A.

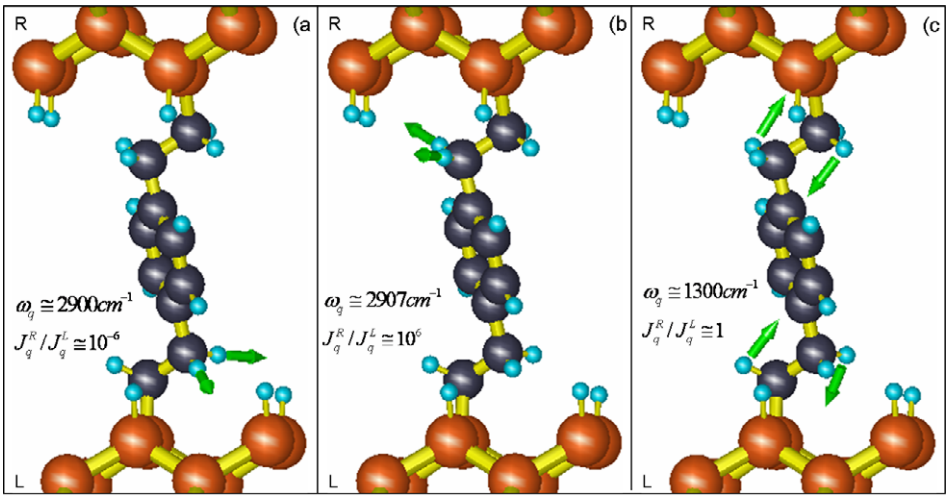

Figure 5. Mode localized near (a) the left contact, (b) the right contact and (c) symmetric on both contacts.

The localization of the modes is another important parameter that governs the decay rates into the contacts. In general, even when the contacts are identical and the bonds of the molecule to the surfaces are the same (as in our case) the decay rate of the molecular vibrons in the two leads can differ significantly. Indeed, the decay rates depend on the localization of the vibrational modes. For instance, consider the vibrational mode of structure A at $\omega_q \cong 2900$ cm^{-1}. This is mainly localized on one side of the molecule, as shown in figure 5(a). As a consequence, the decay rate into the right contact is much higher than the decay rate into the left contact ($J_q^{\mathrm{R}} \gg J_q^{\mathrm{L}}$). In the opposite case, the mode at $\omega_q \cong 2907$ cm^{-1} has a much higher decay rate on the right contact, near which it is localized (see figure 5(b)). Eventually, symmetric modes, such as for instance that at $\omega_q \cong 1300$ cm^{-1}, have an equal decay rate in the two contacts ($J_q^{\mathrm{R}} \cong J_q^{\mathrm{L}}$) (see figure 5(c)). The systems analysed in this paper possess almost perfect inversion symmetry; therefore, for each mode localized near one contact there is an almost degenerate mode localized near the other contact (degeneracy may be left because of a small symmetry breaking due to the numerical geometry optimization). As a consequence the heat release into the two contacts is the same. However, we can envisage that suitably constructed asymmetric molecules may give strongly asymmetric decays, leading to voltage-induced temperature gradients (Peltier effect) or heat rectifiers.

6. Molecular heating

In this section we show the impact of the decay rates, J_q, on the molecular temperature reached under bias conditions. In appendices A and B the essential results of the theory of incoherent transport and molecular heating are reported [19]. Figure 6 shows the coherent current density for both structures at increasing biases. It is possible to see that structure B is much better conducting than structure A. The reason for this pronounced difference is that in structure A the short chains of C_2H_2 represent insulating bridges which are absent in structure B. The Si contacts are made conducting by assuming a degenerate p-doping concentration of 10^{19} holes cm^{-3}. For this reason, at small biases, a larger current is found at energies close to the Si valence band-edge. The peaks appearing within the Si bandgap are related to hybrid molecular states. As the bias above 1.2 V the valence-to-conduction band tunnelling takes

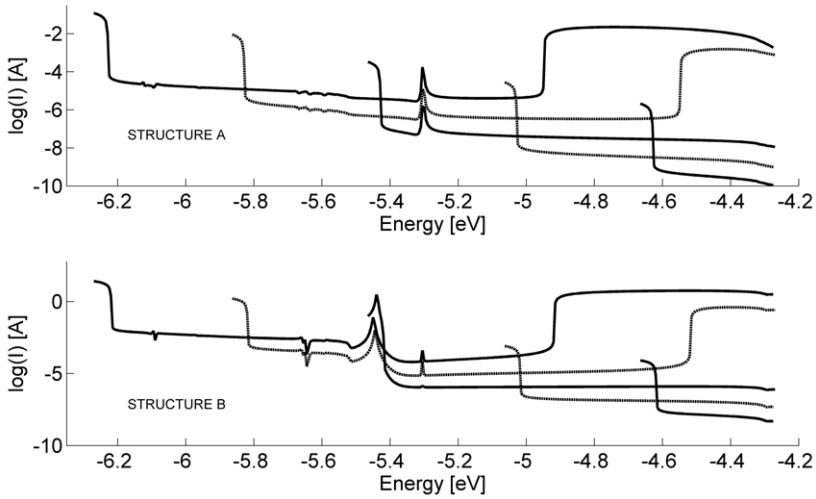

Figure 6. Current density as a function of energy for increasing biases from 0.4 to 2.0 V. The curves are shifted by one order of magnitude for clarity.

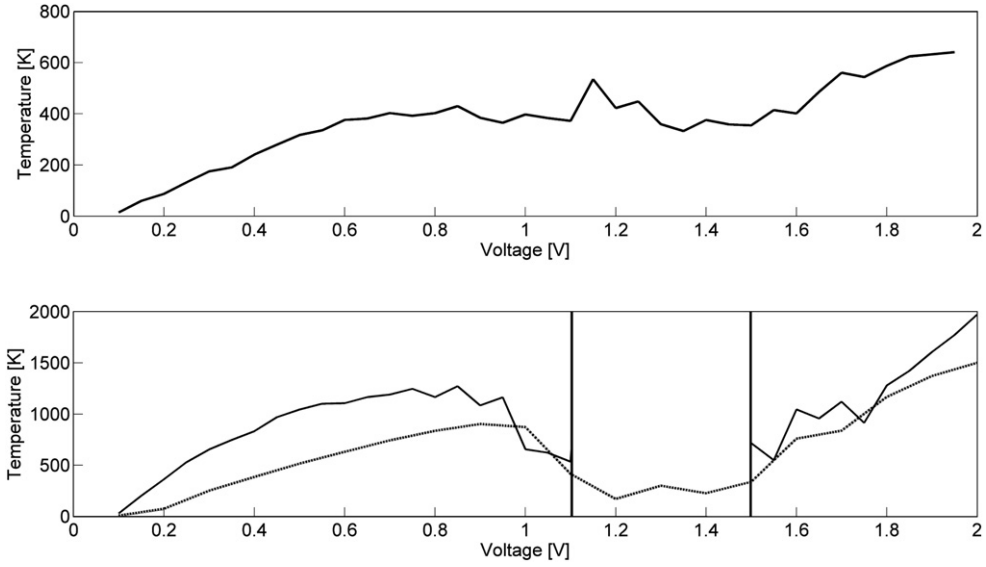

Figure 7. Local temperature reached by the molecules under bias. The upper panel corresponds to structure A, the lower panel to structure B. Solid lines correspond to $p = 10^{19}$ holes cm^{-3}, dotted line to $p = 10^{18}$ holes cm^{-3}. The vertical lines mark an interval where no steady-state solutions are found.

over, leading to an approximately linear increase of current versus voltage. Higher coherent tunnelling is reflected in higher incoherent current, and consequently a higher local heating is generally found for structure B.

The steady-state temperature reached by the two structures under bias conditions is reported in figure 7 as a function of voltage. In this calculation the contact reservoirs are assumed to be at an equilibrium temperature of $T = 0$ K.

The temperature versus bias trend is qualitatively similar in both structures. Initially the temperature steadily increases, up to 0.8 V, then it tends to decrease and increase again above 1.2 V. This particular behaviour is the result of the delicate balance between absorption and emission of phonons and the presence of the Si bandgap. Initially emission is favoured over absorption and the number of excited modes increases with voltage, leading to a constant increase of molecular temperature. In the range 0.8–1.2 V the channel of phonon absorption via valence to conduction band tunnelling opens. This is particularly efficient for modes in the range 1000–1500 cm^{-1}. Since the emission processes are essentially unaffected, the molecular temperature tends to decrease. Above 1.2 V, when the band-to-band tunnelling regime is reached, the emission rapidly increases, particularly in the low-energy modes, leading to a rise of the molecular temperature. Spectroscopic features also play a role, such as for instance the slight peak of temperature found for structure A at 1.15 V, associated to a molecular state also visible in the current density of figure 6.

As anticipated above, structure B tends to heat up much more. In the range between 1.2 and 1.4 V, we even find a bias interval in which no stable steady-state solutions are possible (within the approximations used). In this bias window the molecular distribution of phonons diverges for one or more modes and the molecule is not likely to be stable. The presence of modes with low decay rates due to inefficient coupling with the contacts is crucial in determining this behaviour. From a mathematical point of view, the absence of a steady-state solution is indicated when, for some mode, N_q becomes negative. According to equation (30), instability is found when $J_q + A_q - E_q$ becomes negative for at least one mode. Clearly the value of J_q plays an important role in this calculation, since the stability entirely depends on the difference $A_q - E_q$ for modes with very small J_q. The inclusion of multi-phonon scattering and anharmonic decays may increase J_q, leading to more stable behaviours. Interestingly, for biases larger than 1.4 V the absorption turns to be efficient, compensating the emission, and steady-state solutions are possible. Clearly the bandgap, Fermi level, density of states and electron–phonon coupling interplay in determining this behaviour, according to equations (28) and (29). In order to emphasize this fact we have calculated the temperature behaviour of structure B for a lower doping of the Si contacts of 10^{18} holes cm^{-3}, plotted in the lower panel of figure 7 with a dotted line. In this case the molecular heating is smaller and no instabilities are found because of a generally lower incoherent current density.

7. Conclusions

In this work we have discussed a first-principles method to compute the heat dissipation in molecular electronics, accounting for elastic coupling of localized vibrons with contact phonons. The Green's function formalism gives the theoretical framework in which the projected phonon density of states and the decay rates of the molecular vibrations can be computed. The knowledge of the vibrational lifetimes allow us to set up a rate equation for the phonon dynamics that can be solved self-consistently to find the steady-state distribution of quanta and compute the effective temperature reached by the molecule when a bias is applied. The decay rates are found to be closely related to the phonon bandwidth of the contacts. The method has been applied to two similar systems, showing a different behaviour.

Appendix A

In this appendix we briefly report the essential result of the theory of quantum transport with incoherent electron–vibron scattering presented in [5]. The electron–phonon coupling

Hamiltonian is written in the form

$$H_{\mathrm{el-ph}} = \sum_{q,\mu,\nu} \gamma^{q}_{\mu\nu} c^{\dagger}_{\mu} c_{\nu} \left[a^{\dagger}_{q} + a_{q} \right], \tag{16}$$

by making use of the standard relationships between the position operator and the creation/annihilation phonon operators, $a^{\dagger}_{q}$ and a_{q}, and where $c^{\dagger}_{\mu}$ and c_{ν} are, respectively, the creation and annihilation operators of one electron in the atomic basis. The coupling matrices,

$$\gamma^{\alpha}_{\mu\nu} = \sqrt{\frac{\hbar}{2\omega_q M_q}} \sum_{\alpha} \left[\frac{\partial H_{\mu\nu}}{\partial R_\alpha} - \sum_{\sigma,\lambda} \frac{\partial S_{\mu\sigma}}{\partial R_\alpha} S^{-1}_{\sigma\lambda} H_{\lambda\nu} - \sum_{\sigma,\lambda} H_{\mu\lambda} S^{-1}_{\lambda\sigma} \frac{\partial S_{\sigma\nu}}{\partial R_\alpha} \right] e^{q}_{\alpha}, \tag{17}$$

contain the atomic masses, M_q, the mode frequencies, ω_q, and the normal modes of vibration, e^{q}_{α}. The non-orthogonality of the atomic basis set is reflected by the presence of the overlap matrix, $S_{\mu\nu}$, and its derivative with respect to the ionic positions, R_α.

The electron–phonon interaction is treated within perturbation theory of the non-equilibrium Green's function formalism, and the current through the junction is computed using the Meir–Wingreen formula [20],

$$I = \frac{2e}{h} \int_{-\infty}^{+\infty} \mathrm{Tr} \left[\Sigma^{<}_{\mathrm{L}}(\omega) G^{>}(\omega) - \Sigma^{>}_{\mathrm{L}}(\omega) G^{<}(\omega) \right] \mathrm{d}\omega, \tag{18}$$

where $\Sigma^{<(>)}_{\mathrm{L}}$ represents the injection rate of electrons (holes) from the *left* contact of the device, while $G^{<(>)}$ is the electron (hole) correlation function, obtained from the kinetic equations [21, 22],

$$G^{<(>)}(\omega) = G^{r}(\omega) \Sigma^{<(>)}(\omega) G^{a}(\omega), \tag{19}$$

and $G^{r(a)}$ are the retarded (advanced) Green's functions given by the usual expressions,

$$G^{r(a)}(\omega) = \left[\omega S - H - \Sigma^{r(a)} \right]^{-1}. \tag{20}$$

The *lesser* and *greater* self-energies (SEs) are given by the sum of three terms,

$$\Sigma^{<(>)}(\omega) = \Sigma^{<(>)}_{\mathrm{L}}(\omega) + \Sigma^{<(>)}_{\mathrm{R}}(\omega) + \Sigma^{<(>)}_{\mathrm{ph}}(\omega). \tag{21}$$

The current expressed by equation (18) contains both a coherent and an incoherent component. The coherent component arises from $\Sigma^{<(>)}_{\mathrm{L}}(\omega)$ and $\Sigma^{<(>)}_{\mathrm{R}}(\omega)$, whereas the incoherent component is associated to $\Sigma^{<(>)}_{\mathrm{ph}}(\omega)$, describing scattering processes caused by electron–phonon interactions. The electron–phonon self-energy can be evaluated with diagrammatic techniques. The self-consistent Born approximation (SCBA) is expressed by

$$\Sigma^{<(>)}_{\mathrm{ph}}(\omega) = \mathrm{i} \sum_{q} \int_{-\infty}^{+\infty} \frac{\mathrm{d}\omega'}{2\pi} \gamma_q G^{<(>)}(\omega - \omega') \gamma_q D^{<(>)}_{q}(\omega'), \tag{22}$$

where $D^{<(>)}_{q}$ are the correlation functions related to the vibrational modes,

$$\begin{aligned} D^{<}_{0,q}(\omega) &= -2\pi \mathrm{i} \left[(N_q + 1)\delta(\omega + \omega_q) + N_q \delta(\omega - \omega_q) \right] \\ D^{>}_{0,q}(\omega) &= -2\pi \mathrm{i} \left[(N_q + 1)\delta(\omega - \omega_q) + N_q \delta(\omega + \omega_q) \right], \end{aligned} \tag{23}$$

assumed as Einstein oscillators, i.e. the vibron lifetimes are neglected in the phonon propagator. Inserting (23) into (22), it is possible to derive an explicit form for the electron–phonon self-energy,

$$\begin{aligned} \Sigma^{<}_{\mathrm{ph}} &= \sum_{q} N_q \gamma_q G^{<}(E - \omega_q) \gamma_q + (N_q + 1) \gamma_q G^{<}(E + \omega_q) \gamma_q \\ \Sigma^{>}_{\mathrm{ph}} &= \sum_{q} N_q \gamma_q G^{>}(E + \omega_q) \gamma_q + (N_q + 1) \gamma_q G^{>}(E - \omega_q) \gamma_q. \end{aligned} \tag{24}$$

The self-consistency in equation (22) is implied by the use of a renormalized Green's function, $G^<$, whereas the first-order Born approximation is obtained when the unrenormalized (zeroth-order) Green's function is used to evaluate the electron–phonon self-energy. Using the relationship $\mathrm{Im}[\Sigma^r_{\mathrm{ph}}] = 1/2(\Sigma^>_{\mathrm{ph}} - \Sigma^<_{\mathrm{ph}})$, it is possible to compute Σ^r_{ph}, which modifies the electron propagator in (20). Since we are mainly interested in the electron lifetime and we restrict ourselves to weak electron–phonon coupling, the real part of Σ^r_{ph}, responsible for a polaronic shift, is neglected. Consistently, we also neglect the first-order Hartree diagram, which gives a contribution to the real part only.

Appendix B

In this appendix we briefly report the essential result of the theory of heat dissipation in molecular devices presented in [19]. When a bias is applied to a molecular junction, heat is released in the molecule via incoherent electron–phonon scattering processes. At steady state, the rate of phonons emitted in the junction must balance the rate of phonons dissipated into the heat reservoir. In this model we assume that the two contacts play the role of such reservoirs, and heat release into them is described by the phonon decay rates, J_q. In order to compute the steady-state population of quanta in the molecular degrees of freedom, a semiclassical approach has been followed, by setting a simple rate equation [6],

$$\frac{\mathrm{d}N_q}{\mathrm{d}t} = R_q - J_q\left[N_q - n_q(T_0)\right], \tag{25}$$

balancing the rate, R_q, of quanta emitted, with the decay rate, J_q, into the bath. The first term contains the net emission of phonons into the molecule due to the electron–vibration coupling. The second tends to restore the population to the equilibrium Bose–Einstein distribution, $n_q(T_0)$, characterized by the contact temperature, T_0. At steady state the phonon distribution in the molecule is given by

$$N_q = n_q(T_0) + R_q/J_q. \tag{26}$$

It is possible to demonstrate [19] that

$$R_q = \left[(N_q + 1)E_q - N_q A_q\right], \tag{27}$$

where A_q and E_q can be interpreted to some extent as the phonon emission and absorption rates, given by

$$E_q = \frac{2}{h}\int_{-\infty}^{+\infty} \mathrm{Tr}\left[\gamma_q G^<(\omega+\omega_q)\gamma_q G^>(\omega)\right], \tag{28}$$

and

$$A_q = \frac{2}{h}\int_{-\infty}^{+\infty} \mathrm{Tr}\left[\gamma_q G^<(\omega-\omega_q)\gamma_q G^>(\omega)\right]. \tag{29}$$

Combining equations (30) and (27), it is possible to obtain the out-of-equilibrium number of phonons accumulated in the junction under bias,

$$N_q = \frac{n_q(T_0)J_q + E_q}{J_q + A_q - E_q}. \tag{30}$$

Since the term A_q and E_q depend themselves on the population, N_q, via the Green's function, $G^<$, containing the phonon propagator, a self-consistent loop is necessary.

Once the N_qs are computed, we define an effective molecular temperature, obtained by redistributing the energy stored in the molecular vibrations into a Bose–Einstein distribution,

$n_q(T_{\rm mol})$, with temperature $T_{\rm mol}$. This procedure is equivalent to imposing energy conservation,

$$\sum_q \omega_q n_q(T_{\rm mol}) = \sum_q \omega_q N_q. \tag{31}$$

The definition of the local temperature is a crucial quantity for the analysis of molecular stability.

References

[1] Huang Z, Xu B, Chen Y, Di Ventra M and Tao N J 2006 Measurement of current-induced local heating in a single molecule junction *Nano Lett.* **6** 1240

[2] Galperin M, Nitzan A and Ratner M 2006 Molecular transport junctions: vibrational effects *Preprint* cond-mat/06812085

[3] Todorov T N, Hoekstra J and Sutton A P 2001 Current-induced forces in atomic scale conductors *Phys. Rev. Lett.* **86** 3606

[4] Chen Y C and Di Ventra M 2005 Effect of electron–phonon scattering and shot noise in nanoscale junctions *Phys. Rev. Lett.* **95** 166802

[5] Pecchia A, Gagliardi A, Sanna S, Frauenheim Th and Di Carlo A 2004 Incoherent electron–phonon scattering in octanethiols *Nano Lett.* **4** 2109

[6] Paulsson M, Frederiksen T and Brandbyge M 2005 Modeling inelastic phonon scattering in atomic- and molecular-wire junctions *Phys. Rev.* B **72** 201101(R)

[7] Mingo N and Makoshi K 2000 Calculation of the inelastic scanning tunnelling image of acetylene on Cu(100) *Phys. Rev. Lett.* **84** 3694

[8] Emberly E G and Kirczenow G 2000 Landauer theory, inelastic scattering, and electron transport in molecular wires *Phys. Rev.* B **61** 5740

[9] Ness H and Fisher A J 2002 Coherent electron injection and transport in molecular wires: inelastic tunnelling and electron–phonon interactions *Chem. Phys.* **281** 279

[10] Dong B, Cui H L and Lei X L 2004 Photon–phonon-assisted tunnelling through a single molecule quantum dot *Phys. Rev.* B **69** 205315

[11] Datta S 2000 Nanoscale device simulation: the Green's function formalism *Superlatt. Microstruct.* **28** 253

[12] Guinea F, Tejedor C, Flores F and Louis E 1983 Effective two dimensional Hamiltonian at surfaces *Phys. Rev.* B **28** 4397

[13] Nitzan A, Mukamel S and Jortner J 1973 Some features of vibrational relaxation of a diatomic molecule in a dense medium *J. Chem. Phys.* **60** 3929

[14] Budde M, Lupke G, Cheney C P, Tolk N H and Feldman L C 2000 Vibrational lifetime of bond-centre hydrogen in a crystalline silicon *Phys. Rev. Lett.* **85** 1452

[15] Nitzan A 2006 *Chemical Dynamics in Condensed Phases* (Oxford: Oxford University Press)

[16] Elstner M, Porezag D, Jungnickel G, Elsner J, Haugk M, Frauenheim Th, Suhai S and Seifert G 1998 Self-consistent charge density tight-binding method for simulation of complex materials properties *Phys. Rev.* B **58** 7260

[17] Porezag D, Frauenheim Th, Kohler Th, Seifert G and Kaschner R 1995 Construction of tight-binding-like potentials on the basis of density-functional theory: applications to carbon *Phys. Rev.* B **51** 12947

[18] Frauenheim Th, Seifert G, Elstner M, Hajnal Z, Jungnickel G, Porezag D, Suhai S and Scholz R 2000 A self-consistent charge density functional based tight-binding method for predictive materials simulations in physics, chemistry and biology *Phys. Status Solidi* b **271** 41

[19] Pecchia A, Romano G and Di Carlo A 2006 Theory of heat dissipation in molecular electronics *Phys. Rev.* B **75** 35401-1

[20] Meir Y and Wingreen N S 1992 Landauer formula for the current through an interacting electron region *Phys. Rev. Lett.* **68** 2512

[21] Keldysh L V 1965 Diagram technique for nonequilibrium processes *Sov. Phys.—JETP* **20** 1018

[22] Kadanoff L P and Baym G 1962 *Quantum Statistical Mechanics* (San Francisco, CA: Benjamin)